Inter-Zone Interference Avoidance Using Channel Reservation in Multiple Subcarrier Multiple Access Scheme

Masahiro Otani
The University of Electro-Communications
Tokyo, 182-8585, Japan
otani.masahiro@kwkt-lab.org

Tomoaki Matsuda
matsuda.tomoaki@kwkt-lab.org

Nitish Rajoria
Keio University
Fujisawa, 252-0882, Japan
nitish@keio.jp

Jin Mitsugi
Keio University
Fujisawa, 252-0882, Japan
mitsugi@keio.jp

Haruhisa Ichikawa
The University of Electro-Communications
Tokyo, 182-8585, Japan
h.ichikawa@inf.uec.ac.jp

Yuusuke Kawakita
The University of Electro-Communications
Tokyo, 182-8585, Japan
kwkt@inf.uec.ac.jp

ABSTRACT

Interest in structural health monitoring for which sensors are used to detect structural damage has increased. For low-cost installation, these sensors are required to be batteryless and wireless. The objective of this study is to realize structural health monitoring for large-scale structures using a multiple subcarrier multiple access scheme that functionally enhances sub-carrier methods in radio-frequency identification (RFID) communication. When the target structure is of large scale, it is necessary to divide the structure into several zones because of communication distance restrictions. In this case, some wireless sensor nodes are located in zones where adjacent transceiver ranges overlap, thereby transmitting their sensing signals to both zones; thus, the problem of inter-zone interference due to unintended subcarriers arises. Therefore, we propose a method of inter-zone interference avoidance in which channels are reserved for wireless sensors overlapping adjacent zones. Evaluation via simulation reveals that the average communication capacity reduction can be suppressed compared with the case without channel reservation.

ACM Classification Keywords

C.2.1 Network Architecture and Design: Wireless communication; C.2.5 Local and Wide-Area Networks: Access schemes

Author Keywords

Multiple access; RFID; Interference prevention; Channel allocation

IoT 2017, October 22–25, 2017, Linz, Austria

ISBN 978-1-4503-5318-2/17/10...$15.00

DOI: https://doi.org/10.1145/3131542.3131546

INTRODUCTION

Items of social infrastructure such as tunnels and bridges are aging continuously, and the number of structures that require inspection is, therefore, increasing. However, the costs of such examinations are extremely high and, thus, there is significant demand for an efficient and low-cost inspection technique. Hence, structural health monitoring[1], a technique to examine structural damage using various sensors, has attracted considerable research attention, leading to the development of various methods [2]-[5].

In large-scale structural health monitoring, it is unrealistic to communicate with or supply power to each sensor via wiring; thus, the sensor nodes should be wireless. Further, battery-driven sensors experience power supply limitations when used for communication and sensing. To overcome this problem, wireless sensors with applied passive radio-frequency identification (RFID) systems have been developed [6]-[8]. A passive RFID system consists of an RF tag and RF reader/writer. The RF tag uses backscatter communication and reflects a modulated signal in response to a carrier transmitted by the RF reader/writer. Further, an RF tag can be manufactured at low cost. Thus, it can be expected that structural health monitoring can be conducted by embedding sensors with a passive RFID system into a large structure.

Generally, the multiple access scheme used in the RFID system is time division multiple access (TDMA); however, it is difficult to implement synchronization between multiple points in this approach. Although time synchronization methods have been suggested, such as the flooding time synchronization protocol (FTSP) [9], wireless sensors must communicate to achieve time synchronization, which involves considerable battery consumption. Previously, the authors proposed multiple subcarrier multiple access (MSMA), which expands RFID communication uniquely [10]. MSMA enables asynchronous communication via multiple subcarriers, but has only been evaluated for a single zone to date. However, a large structure

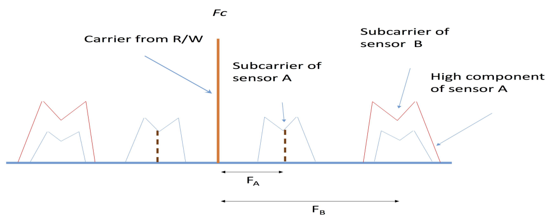

Figure 1. Interference caused by harmonics on other subcarriers in multiple subcarrier multiple access

must be divided into several zones because of the communication distance restriction.

The purpose of this study is to realize batteryless wireless structural health monitoring, focusing in particular on interference avoidance for the multiple zones in MSMA. This topic has been rarely studied. In the case where sensors are positioned in zones where adjacent transceiver ranges overlap, these sensors transmit subcarriers to both zones. Then, careless channel allocation causes unintended interference. Here, a method of avoiding inter-zone interference is discussed. The remainder of the paper is organized as follows: In Sect. 2, we introduce an overview of MSMA and discuss scenarios in which inter-zone interference occurs. In Sect. 3, the proposed method of inter-zone interference prevention is suggested. In Sect. 4, we evaluate the results of simulations and we conclude the paper in Sect. 5.

MULTIPLE SUBCARRIER MULTIPLE ACCESS (MSMA) AND INTER-ZONE INTERFERENCE

Overview of MSMA

As subcarriers generate harmonic components on odd multiples of the original subcarrier frequency, a single subcarrier is considered in international standards [11]. However, MSMA is a type of multiple access method that enables asynchronous stream communication using multiple subcarriers. Therefore, the harmonic components of subcarriers may interfere with the other subcarriers, as illustrated in Fig. 1. Even if interference occurs, however, the signals can be recovered through successive interference cancellation, provided the subcarrier channel allocation is known.

Assuming that the number of wireless sensors is equivalent to the number of available subcarriers, the relationship between the transmission signals of the wireless sensors and the signals received from the RF reader/writer is expressed in the following matrix equation:

$$\begin{Bmatrix} R_1 \\ R_2 \\ R_3 \\ \vdots \\ R_9 \\ \vdots \end{Bmatrix} = \begin{bmatrix} 1 & 0 & 0 & 0 & \cdots \\ 0 & 1 & 0 & 0 & \cdots \\ \frac{1}{3} & 0 & 1 & 0 & \cdots \\ \vdots & & & & \cdots \\ \frac{1}{9} & 0 & \frac{1}{3} & 0 & \cdots \\ \vdots & & & & \ddots \end{bmatrix} \begin{Bmatrix} T_1 \\ T_2 \\ T_3 \\ \vdots \\ T_9 \\ \vdots \end{Bmatrix}. \tag{1}$$

Here, R_i represents the signal received on subcarrier channel i and T_i represents the original transmission signal of the wireless sensor on subcarrier channel i. Eq. 1 is a lower triangular matrix and the original wireless sensor signal can be expressed in forward catenation as

$$\begin{aligned} T_1 &= R_1, \\ T_2 &= R_2, \\ T_3 &= R_3 - \frac{1}{3}R_1, \\ T_9 &= R_9 - \frac{1}{9}R_9 - \frac{1}{3}R_3. \end{aligned} \tag{2}$$

Subcarrier Allocation Scheme

In an MSMA scheme, harmonic components of the subcarrier signal theoretically occur on odd multiples of the subcarrier frequency. Further, the signal that is closest to the carrier frequency generates more interference than the other subcarriers. Therefore, fairness among the mutual wireless sensors must be considered during subcarrier channel allocation.

Previously, four subcarrier channel allocation schemes were compared in Ref. [12], and the average communication capacity and fairness were evaluated. In addition, an allocation scheme named "farthest tag nearest subcarrier (FTNS)" was proposed in Ref. [12]. The interference strength of a given harmonic component depends on the strength of the original subcarrier, with the subcarrier closer to the carrier frequency generating greater interference than the other subcarriers, as described above. Therefore, FTNS allocates channels close to the carrier frequency to the farthest sensors in descending order; this means that the signals received from those sensors are weak. In this paper, FTNS is used to evaluate the proposed methodology.

Communication Capacity of MSMA scheme

The communication capacity of the MSMA scheme is calculated from Shannon's theorem. Assuming that the bandwidth of each subcarrier is B, the communication capacity c_i of the ith subcarrier is expressed as

$$c_i = B\log_2(1 + SINR_i). \tag{3}$$

Here, $SINR_i$ is the signal-to-interference-noise ratio of the ith wireless sensor. The power loss of the transmission signal includes the free space loss and backscatter attenuation. We use the Friis transmission equation to determine the free space loss and set the backscatter attenuation to 90%.

The interference power H_{ij} given to subcarrier j by a wireless sensor assigned the ith subcarrier channel is expressed as follows, using the received signal strength S_i:

$$H_{ij} = \begin{cases} i\frac{S_i}{j}, & if(mi = j, m = 3,5,7\cdots), \\ 0, & if(mi \neq j). \end{cases} \tag{4}$$

As the harmonic components interfering with subcarrier j are generated from the subcarriers to the 3 / j channel, the sum of the interference power is expressed as

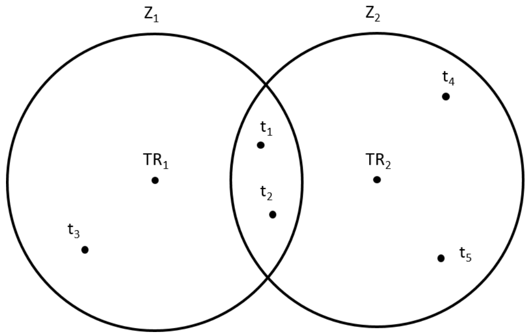

Figure 2. Conceptual diagram of wireless sensing system for multiple sensing zones

$$H_j = \sum_{i=1}^{\lfloor j/3 \rfloor} H_{ij}. \tag{5}$$

In addition, thermal noise is assumed as the cause of the interference, being given by $n_T = kTB$. In this equation, n_T, k, T, and B represent the thermal noise (W), the Boltzmann constant (J/K), the temperature (K), and the bandwidth (Hz).

The sum of the communication capacity C using the above definitions is expressed as

$$C = \sum_{i=1}^{N} c_i = \sum_{i=1}^{N} B \log_2(1 + SINR_i), \\ = \sum_{i=1}^{N} B \log_2(1 + \frac{S_i}{H_i + n_T}). \tag{6}$$

Further, the average communication capacity of the entire system is the quotient obtained by dividing C by the total number of sensors N.

Inter-zone Interference

In MSMA, when the wireless sensor nodes are positioned such that their ranges overlap in adjacent zones, each of these sensors transmits the sensing signal for the carrier to both zones. Even if the subcarrier frequencies in adjacent zones are set far apart, this interference is inevitable. A conceptual diagram of an MSMA communication system featuring two sensing zones is shown in Fig. 2. We label the communication range of a transceiver as zone Z, a wireless sensor node as t, and a transceiver with RFID reader/writer functionality as TR. Thus, in Fig. 2, wireless sensor nodes t_1 and t_2 exist in the area where the TR_1 and TR_2 zones overlap. The wireless sensor subcarriers existing in Z_1 and Z_2 are allocated channels by TR_1 or TR_2 so that the same channel is not used twice within a zone, and the channels are assumed to be known for each zone. We assume that t_1 and t_2 (located in the overlap zone) are allocated channels as sensors belong to Z_1, and that each center frequency of the carriers used in each zone is known. In addition, the subcarrier channel allocated by the transceiver is labeled Sch.

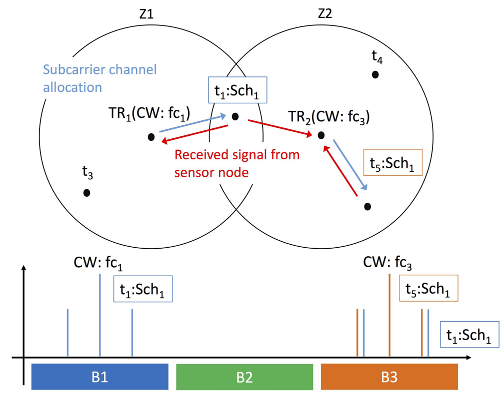

Figure 3. Inter-zone interference for multiple subcarrier multiple access scheme

Using Eq. 2, replica signals can be calculated from the first subcarrier. Then, successive interference cancellation is conducted by subtracting the harmonic components from the channel for which interference occurs.

However, a problem can arise, as shown in Fig. 3. That is, t_1 located in the overlap zone is assigned Sch_1 as part of Z_1 , but t_5 in Z_2 is also assigned Sch_1. In this case, TR_2 cannot conduct successive interference cancellation and obtain a receiving signal on the Sch_1 from t_5. Thus, if sensors are positioned in a region where adjacent transceiver zones overlap, interference caused by these sensors occurs, which is called inter-zone interference.

PROPOSED METHOD TO PREVENT INTER-ZONE INTERFERENCE

In this section, the proposed methodology to avoid inter-zone interference is introduced. First, we explain the basic features of the proposal. Then, the subcarrier-channel allocation scheme using the RFID system is clarified.

The proposed method aims to prevent duplication of the subcarrier channels by reserving assigned channels for allocation to sensors positioned in the overlap regions of adjacent transceiver zones. First, we obtain the sensors in each zone. Next, the sensors in one of the zones is allocated channels. Simultaneously, the TR in the other, adjacent zone reserves channels for the sensors in the overlap zone while unreserved channels are allocated to the other sensors.

We assume the reader/writer receives streaming signals from the sensor nodes without synchronization between the sensor nodes. Fig. 4 shows the subcarrier channel allocation achieved using the RFID system. The transceivers are controlled by the management node. First, the management node sends an inventory command to TR_1 in order to assign subcarrier channels to the Z_1 sensors. TR_1 receives the inventory command and executes inventory in Z_1, listing the sensors. Likewise, the management node also obtains a list of the sensors in Z_2 and acquires the sensor nodes in the overlap region of both zones. In Fig. 4, t_2 is an example of an overlap node.

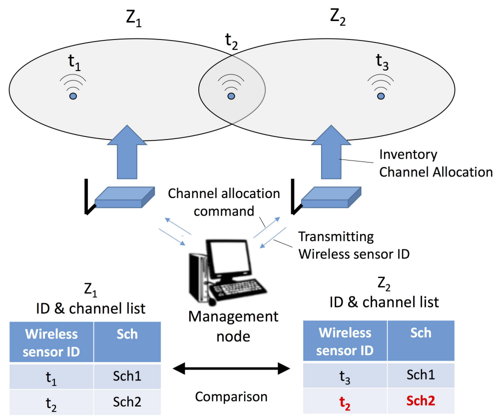

Figure 4. Subcarrier channel allocation procedure using RFID system

Table 1. Parameters used in simulation for two adjacent zones

Subcarrier channel allocation scheme	FTNS
Carrier frequency	920 MHz
Transceiver transmission power	1 W
Transceiver coordinates [x, y]	TR_1: [0, 0], TR_2: [16, 0]
Subcarrier bandwidth	1 kHz
Number of wireless sensors	50
Number of wireless sensor in inter-zone	0, 10, 20, 30, 40, 50
Location range of wireless sensors	Circle with 10-m radius centered on TR_1 or TR_2

The management node allocates channels to the sensors in Z_1 as the set method. Simultaneously, Sch_2 is reserved and allocated to sensor node t_2, which is in the overlap region of both zones. For the channel allocation of the sensors in Z_2, channels other than the reserved channels are used.

SIMULATION RESULTS

To evaluate the proposed method, we calculated the communication capacities of two different systems (i.e., with two and three zones) via a MATLAB simulation. Note that it was difficult to conduct a simulation with existing network simulators such as QualNet and COOJA, because MSMA is a communication method that enhances the global standard of RFID [11]. Although inter-zone interference can be avoided using the proposed method, the communication capacity may decrease in the adjacent zone, because fewer interference channels cannot be used as a result of the channel reservation. Therefore, it was expected that the communication capacity of the adjacent zone would be lower than that of the single-zone case. To examine this behavior, we compared cases with and without channel reservation for multiple zones.

There are three classes of sensor allocation, one-, two-, and three-dimensional allocation. In this study, we conducted a simulation in the two-dimensional allocation class. The parameters used in the two-zone simulation are listed in Table

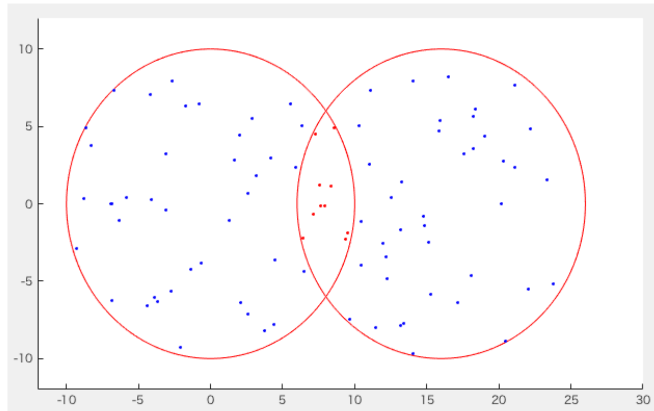

Figure 5. Sample wireless sensor distribution for two adjacent zones ($N = 50$)

1. The coordinates of TR_1 and TR_2 were set to [x,y] = [0,0] and [0,16], respectively. The region within a 10-m radius of each transceiver was defined as the transmission zone of that receiver. The number of sensors N in one zone was set to 50. As the simulation procedure, N_v sensors were randomly placed in $Z_1 \cap Z_2$ and the remaining sensors were placed in $\neg Z_1 \cap Z_2$. A sample sensor-node distribution is shown in Fig. 5 and the allocation procedure is shown in Algorithm 1.

Algorithm 1 Sensor allocation

ZoneN is the number of zones.
$i = 1$;
while $i \leq ZoneN$ **do**
  if $i \neq ZoneN$ **then**
    Allocate sensors on $Z_i \cap \neg Z_{i+1}$
    Allocate sensors on $Z_i \cap Z_{i+1}$
  else
    Allocate sensors on $\neg Z_{i-1} \cap Z_i$
  end if
  $i = i + 1$;
end while

We assumed that the number of available subcarrier channels was equal to the total number of sensor nodes. The subcarrier channel allocation of Z_1 was performed initially, with no reserved channels. Thus, the channel assignment of Z_1 is identical to that for the single-zone case.

The communication capacity calculation procedure is as shown in Algorithm 2. The communication capacities of Z_1 (equivalent to a single zone), Z_2 (with channel reservation), and Z_2 (no reservation) were determined in detail. In Z_1, channel allocation was executed using FTNS based on the distance between the wireless sensors and TR_1. In Z_2 (with reservation), channels were reserved for sensors in $Z_1 \cap Z_2$. The sensors belonging to $\neg Z_1 \cap Z_2$ were allocated unreserved channels close to the carrier frequency in order of distance from TR_2. In Z_2 (no reservation), no channels were reserved for the sensors in $Z_1 \cap Z_2$. The sensors positioned within $\neg Z_1 \cap Z_2$ were allocated unreserved channels close to the carrier

Algorithm 2 Communication capacity calculation

ZoneN is the number of zones.
CC_N is the set of average communication capacities of each zone sensor.
$i = 1$;
while $i \le ZoneN$ **do**
  if $i = 1$ **then**
    Allocate channels to sensors on Z_i with FTNS
    Calculate signal strength of each sensor on Z_i with free space loss
    Calculate communication capacity of each sensor on Z_i
    $CC_i \Leftarrow$ average communication capacity of sensors on Z_i
  else
    Allocate channels to sensors on $\neg Z_{i-1} \cap Z_i$, excluding those used in $Z_{i-1} \cap Z_i$
    Calculate signal strength of each sensor on Z_i with free space loss
    Calculate communication capacity of each sensor on Z_i
    $CC_i \Leftarrow$ average communication capacity of sensors on Z_i
  end if
end while

frequency in order of distance from TR_2. The signals S_i of the sensor nodes within $Z_1 \cap Z_2$ and $\neg Z_1 \cap Z_2$ were calculated. When calculating H_j, the S_i of sensors in $Z_1 \cap Z_2$ were treated as interference sources affecting the sensors in $\neg Z_1 \cap Z_2$ and were added to H_j if duplication of allocated channels occurred.

The above operations were simulated 100 times with N_v changing in 5 increments, for cases both with and without channel reservation. The simulation results are shown in Fig. 6. For $N_v = 0$, there is little difference between Z_1, Z_2 (with reservation), and Z_2 (no reservation) as regards the average communication capacity. However, as Nv increases, the communication capacity of Z_1 decreases. This behavior can be interpreted as being due to the increased free space loss as the number of sensor nodes located on the overlap zone far from the transceiver increases. As regards the other two cases (Z_2 with and without channel reservation), as N_v increases, channels with many interference components are used for allocation and the average communication capacities decrease. For Z_2 (no reservation), a significant decrease in communication capacity can be confirmed as Nv increases compared with Z_2 (with reservation). For example, in the case of $Nv = 30$, Z_2 (no reservation) is reduced to 52% of the average communication capacity of Z_1, whereas Z_2 (with reservation) retains 95% of the average communication capacity.

Next, a simulation involving three adjacent zones was performed. The coordinates of TR_1, TR_2, and TR_3 were set to [x,y] = [0,0], [0,16], and [0,32], respectively. Again, the area within a 10 m radius of each transceiver was defined as the transmittable area and N was set to 50 for each zone. The numbers of sensor nodes located in $Z_1 \cap Z_2$ and $Z_2 \cap Z_3$ were labeled N_{v1} and N_{v2}, respectively, and both N_{v1} and N_{v2} were

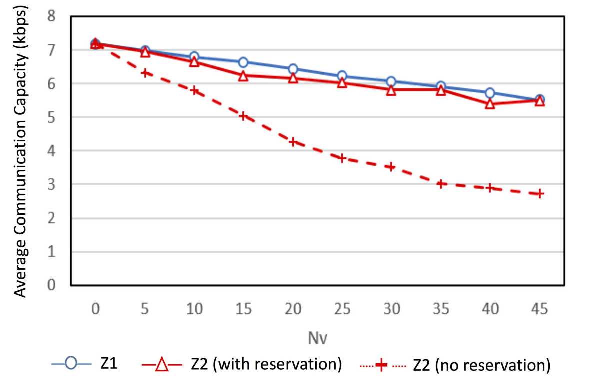

Figure 6. Relationship between number of wireless sensors in adjacent-zone overlap region and average communication capacity (two adjacent zones)

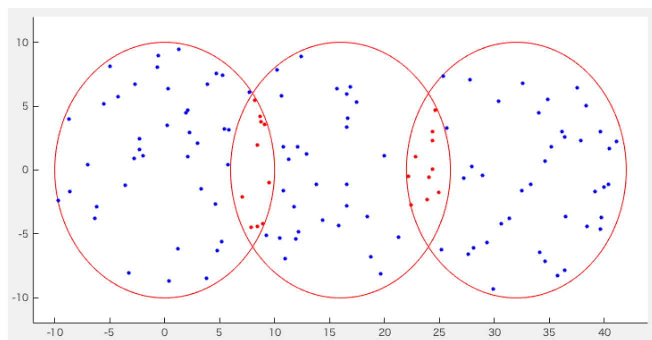

Figure 7. Sample wireless sensor distribution for three adjacent zones ($N = 50$)

varied during the simulations. As regards the sensor-node distribution, the N_{v1} sensors were first placed in $Z_1 \cap Z_2$, $50 - N_{v1}$ sensors were then placed in $Z_1 \cap \neg Z_2$, N_v2 sensors were then placed in $Z_2 \cap Z_3$, $50 - N_{v1} - N_{v2}$ sensors were then placed on $\neg Z_1 \cap Z_2 \cap \neg Z_3$, and $50 - N_{v2}$ sensors were placed on $\neg Z_2 \cap Z_3$. An sample sensor-node distribution is shown in Fig. 7. Sensors in $Z_1 \cap Z_2$ and $Z_2 \cap Z_3$ were assigned subcarrier channels by TR_1 and TR_2, respectively. The other parameters are listed in Table 1.

The above operations were simulated 100 times with and without channel reservation, for $N_{v1} = 10$ and $N_{v2} = 0$–40, and for $N_{v1} = 20$ with $N_{v2} = 0$–30. Note that N_{v2} was adjusted in increments of five. These results are shown in Figs. 8 and 9.

When N_{v1} is 10 (Fig. 8), there is little difference between Z_1, Z_2 (with reservation), and Z_3 (no reservation) as regards the average communication capacity at $N_{v2} = 0$. When the value of N_{v2} is varied, the communication capacity of Z_2 (no reservation) is approximately 1 kbps lower than that of Z_2 (with reservation). The reason for this behavior is thought to be that N_{v1} is fixed to 10. Further, it is confirmed that the communication capacity of Z_3 (no reservation) is substantially lower than that of Z_3 (with reservation) as N_{v2} increases. For instance, when $N_{v2} = 30$, Z_3 (no reservation) is reduced to 43% of the average communication capacity of Z_1, whereas Z_3

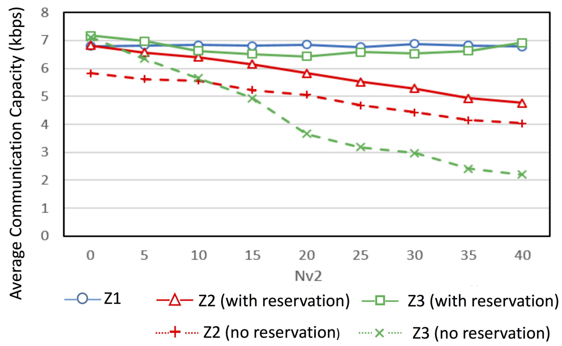

Figure 8. Relationship between number of wireless sensors in adjacent-zone overlap region N_{v2} and average communication capacity (with N_{v1} = 10 fixed)

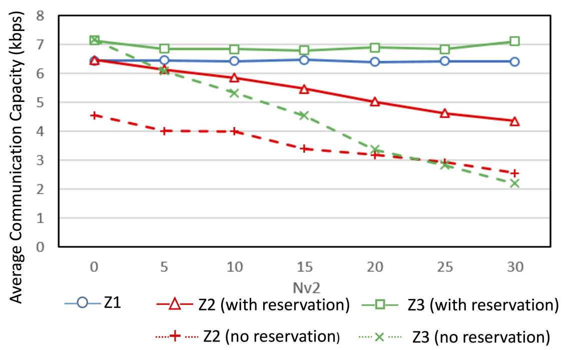

Figure 9. Relationship between number of wireless sensors in adjacent-zone overlap region N_{v2} and average communication capacity (with N_{v1} = 20 fixed)

(with reservation) retains 95% of the average communication capacity.

CONCLUSION

In this paper, structural health monitoring through the construction of a dense wireless sensor network on a large-scale structure was considered. To achieve such monitoring, MSMA, which enhances the subcarrier communication method used in the passive RFID communication system, is required. However, in such a setup, sensors positioned in overlap regions between adjacent transceiver zones transmit sensing signals to transceivers in either zone causing inter-zone interference; this behavior must be avoided. Therefore, we proposed a methodology to prevent this interference, in which the channels used by sensors in overlap regions of adjacent zones are reserved. Simulation results indicated that, when channel reservation was implemented, the decrease in the average communication capacity could be suppressed compared with the case in which channel reservation was not implemented. For example, in the case of two adjacent zones and where the number of sensors in the overlap region was 30, the average communication capacity of the second zone (no reservation) was reduced to 52% of that of the first zone. However, the communication capacity of the second zone (with reservation) remained at 95% of that of the first zone. This simulation covered the class in which sensors are placed on a two-dimensional area without external interference or multi-path fading. Such two-dimensional allocation can be applied to road structures, whereas a three-dimensional allocation can be applied to more general structures. Simulation in three dimensions and comparative analysis with the present study are targets for future works.

ACKNOWLEDGMENTS

This research and development work was supported by the MIC/SCOPE #155003007.

REFERENCES

1. Noel A., Abdaoui A., Badawy A., Elfouly T., Ahmed M., & Shehata M. (2017). Structural Health Monitoring using Wireless Sensor Networks: A Comprehensive Survey. *IEEE Communications Surveys & Tutorials* (2017) 1403 - 1423 .
2. David E. Culler and Hans Mulder. 2004. Smart sensors to network the world. *Scientific American* 290, 6 (2004), 85.
3. Vehbi C. Gungor and Gerhard P. Hancke. 2009. Industrial wireless sensor networks: Challenges, design principles, and technical approaches. *IEEE Transactions on Industrial Electronics* 56, 10 (2009), 4258-4265
4. Jerome P. Lynch and Kenneth J. Loh. 2006. A summary review of wireless sensors and sensor networks for structural health monitoring. *Shock and Vibration Digest* 38, 2 (2006), 91-130.
5. Simon Laflamme, Matthias Kollosche, Jerome Connor, and Guggi Kofod. 2012. Soft capacitive sensor for structural health monitoring of large-scale systems. *Structural Control and Health Monitoring* 19, 1 (2012), 70-81.
6. Prasanna Kalansuriya, Rahul Bhattacharyya, Sanjay E. Sarma, and Nemai Chandra Karmakar. 2012. Towards chipless RFID-based sensing for pervasive surface crack detection. In *Proceedings of RFID-Technologies and Applications (RFID-TA), 2012 IEEE International Conference on.* IEEE, 46-51.
7. Rahul Bhattacharyya, Christian Floerkemeier, and Sanjay Sarma. 2010. Low-cost, ubiquitous RFID-tag-antenna-based sensing. In *Proceedings of the IEEE*, 98, 9, (2010), 1593-1600.
8. Vamsi Talla and Joshua R. Smith. 2013. Hybrid analog-digital backscatter: A new approach for battery-free sensing. In *Proceedings of RFID (RFID), 2013 IEEE International Conference on.* IEEE, 74-81.
9. Miklós Maróti, Branislav Kusy, Gyula Simon, and Ákos Lédeczi. 2004. The flooding time synchronization protocol. In *Proceedings of the 2nd International Conference on Embedded Networked Sensor Systems*, (2004), 39-49.
10. Yuki Igarashi, Yuki Sato, Yuusuke Kawakita, Jin Mitsugi, and Haruhisa Ichikawa. 2014. A feasibility study on simultaneous data collection from multiple sensor RF tags with multiple subcarriers. *RFID (IEEE RFID), 2014 IEEE International Conference on.* IEEE, 141-146.

11. EPC radio-frequency identity protocols specification for RFID air interface protocol for communications at 860 MHz - 960 MHz version 2.0.0 ratified. http://www.gs1.org/sites/default/files/docs/epc/uhfc1g2_2_0_0_standard_20131101.pdf.

12. Nitish Rajoria, Yuki Igarashi, Jin Mitsugi, Yuusuke Kawakita, and Haruhisa Ichikawa. 2015. Comparative analysis on channel allocation schemes in multiple subcarrier passive communication system. *IEICE Transactions on Communications* 98, 9 (2015), 1777-1784.